Optimal mould design for the manufacture by compression moulding of high-precision lenses

M. Sellier[†] [1], C. Breitbach[†], H. Loch[†] and N. Siedow[‡]

August 7, 2006

[†] Schott AG, Hattenbergstrasse 10, 55122 Mainz, Germany
[‡] Fraunhofer-Institut fuer Techno- und Wirtschaftsmathematik (ITWM)
Fraunhofer-Platz 1, 67663 Kaiserslautern, Germany

Abstract

The increasing need for low-cost, high-precision optical devices requires innovative manufacturing techniques or the optimization of existing ones. The present study focuses on the latter alternative and proposes a computer-aided, mould optimization algorithm for the manufacturing of high-precision glass lenses by compression moulding. The intuitive, yet very efficient, algorithm computes at each optimization loop the mismatch between the desired and deformed glass shapes and uses this information to update the mould design. To solve this optimal shape design problem, a finite element model representative of the real industrial process is developed and solved in the commercial package ABAQUS. This model solves the several stages involved in the process and includes the thermo-mechanical coupling, the varying mechanical contact between the glass and the mould, and the stress and structure relaxation in the glass. The algorithm is successfully tested for the mould design for a plano-concave and a bi-concave lens as the residual error between the deformed and desired glass profiles is decreased to a value of the order of one micron.

Keywords: optimal shape design, compression moulding, glass forming, finite element model.

[1] mathieu.sellier@itwm.fhg.de

1. Introduction

In the competitive industry of optics manufacturing, there is a growing need for the mass production of high-precision glass parts. To date, however, there is still a conflict between the productivity and accuracy requirements. Indeed, existing techniques relying on the grinding and polishing of the moulded glass piece can achieve sub-micron accuracy but at a prohibitive cost. A much more time- and cost-effective alternative would be to predict directly the mould design which yields the net, desired glass shape at the end of the forming process without requiring further post-processing.

The compression moulding process, illustrated in Figure 1, consists of three stages: heating of the glass preform/mould assembly to a temperature above the glass transition temperature, pressing of the softened glass to transfer the mould shape onto the glass and, cooling down to room temperature. The mould design in this process is a challenging task because of the deformations induced during cooling stage (thermal shrinkage, residual stresses). Although the profile of the mould might be perfectly transferred to the softened glass at the end of the pressing stage, a strategy is required to compensate for these deformations. Existing compensation techniques rely, according to Yi and Jain in [1], on a simple first-order theory of thermal expansion but such an approach comes to a limit when accuracy of the order of one micron is targeted. Other studies related to the computer-aided tool design for glass forming include, for example, that of Moreau *et al.* in [2] who optimize the press design in the forming of an automotive rear side panel, that of Lochegnies *et al.* in [3] who determine the required mould yielding a prescribed glass thickness distribution in the blow and blow process, or that of Agnon and Stokes in [4] who derive the former shape that produces a prescribed top surface curvature profile in the thermal replication process.

The aim of the present work is to present a numerical algorithm to optimize the mould shape in the context of high-precision compression moulding and demonstrate its ability to produce challenging lens designs with an accuracy of the order of one micron. The intuitive idea of the algorithm is to iteratively "test and correct". The residuals giving a measure of the mismatch between the final and desired glass piece geometries are computed at each optimization loop and used to update the previous mould design.

The next section is devoted to the description of the process and its modelling in the finite element package ABAQUS. The details of the computer-aided mould optimization algorithm follow. Lastly, results supporting the success of the method for the mould design for a plano-concave and a bi-concave lens shape are reported.

2. Modelling of the process

The first requirement to tackle numerically the optimal shape design problem described above is to be able to model accurately the forward problem, i.e. "what is the final glass profile for a given mould design?" Modelling the entire process is a complicated task because of the many stages involved, the thermo-mechanical coupling, the varying mechanical contact between the glass and the mould, and the complex rheology of the glass. To reduce the computational cost, only a simplified model representative of the whole industrial process is considered. The model is solved in the commercial finite element package ABAQUS and user-defined subroutines were developed to implement the complex rheology of the glass. Since the forming temperature is slightly above the glass transition temperature, the glass is in the viscoelastic range and the combined effects of stress and structure relaxation must be accounted for in order to achieve the necessary accuracy. The glass behaviour is represented by the Tool-Narayanaswamy model, [5, 6]. This model has become a standard to handle stress relaxation in glassy materials under non-isothermal conditions. The interested reader is referred to [8] for a thorough description of the model and to [7] for an overview. It suffices here to say that the glass has a transition temperature of 505 °C. Other glass properties and relaxation parameters are not reported since the optimization method described is entirely based on geometric considerations and its success is therefore independent of the precise material properties or operating conditions. The mould is modelled in ABAQUS as a rigid body since its stiffness is much greater than that of the glass.

The finite element analysis is restricted to an axisymmetric geometry and only a two-dimensional radial cross section of the model is represented in Figure 2 for the plano-concave lens and in Figure 3 for the bi-concave one. The glass preform is enclosed in the upper and lower parts of the mould and the outer ring prevents it from flowing outwards during the pressing stage. The outer ring is simply represented in ABAQUS by a rigid surface since its influence on the overall process is minor. In the real industrial process, the glass preform is produced in a low-cost, low-precision, preliminary stage with a near optimal shape and volume. For the plano-concave case, the preform has a flat lower surface and a spherical, concave upper one of radius of 44 mm. This radius is 10% greater than that of the desired final lens design (40 mm). For the bi-concave lens design, the upper and lower preform surfaces are both spherical and concave with a radius of 44 mm which is again 10% greater than the radii of the desired lens design.

The thermo-mechanical coupling is included in the three stages of the transient analysis (heating, pressing, and cooling) but the effects of radiative heat transfer are neglected. The required symmetry conditions are imposed along the axis and the nodal vertical displacements are prescribed to vanish on the lower side of the lower mould (see the boundary conditions on the left-hand side of Figures 2 and 3).

The glass and both parts of the mould are initially in contact along the axis. Thermal boundary conditions of the Dirichlet-type are applied on the top of the upper and the bottom of the lower mould and the lateral walls of the moulds are assumed to be insulated. All other boundaries are grouped in contact pairs. For the two surfaces of a contact pair, which don’t necessarily have to be in contact, mechanical and thermal surface interaction models are defined. In this set-up two nodes of the contact pair surfaces 1 and 2 exchange heat fluxes per unit area taking into account surface to surface radiation and heat conduction through the air layer between the two surfaces.

The heating stage consists of imposing a steadily increasing temperature on the upper side of the upper mould and the lower side of the lower one (time-dependent Dirichlet boundary conditions). The temperature rises from 50 °C to 600 °C in 180 s and then remains constant for 180 s to reach a uniform temperature field. This temperature is about 95 °C above the glass transition temperature, a sufficiently high temperature to shape the glass preform. During this stage, the upper mould is moved upwards by a small amount to allow the glass to expand freely.

In the pressing stage, the temperature is held constant at 600 °C and a downward stroke is imposed on the upper mould. The value of the displacement is chosen so that the lens thickness at the centreline is equal to the desired one. The displacement is ramped linearly in a time interval of 360 s. At the end of the pressing stage, the mould shape is transferred onto the mould.

Finally, the temperature at both ends of the glass and mould assembly is decreased from 600 °C to 20 °C in 360 s during the cooling stage. This steady cooling is followed by a period of 180 s during which the temperature is kept at 20 °C. The position of the mould is held constant during this stage and a gap between the glass and the mould appears and grows because of the thermal shrinkage and the residual stresses in the glass. The right-hand side of Figures 3 and 4 shows the glass/mould assembly at the very end of the forming process when the desired glass profile is given to the mould. Although the magnitude of the gap is small in magnitude, the consequent mismatch between the contour of the glass piece and the one of the closed mould needs to be compensated for if an accuracy of the order of one micron is targeted.

3. Description of the mould optimization algorithm

The optimization algorithm described in the following ignores the very details of the compression moulding process. It simply considers it as an operator F which maps the initial mould contour C_m^j into the final glass shape C_g^j at iteration j (see Figure 4). Although the glass contour is a closed curve, the upper and lower curves are considered independently in the range $[0, r_i]$. The curves are represented, in the scientific computing program MATLAB, by cubic splines fitted through the nodes of the mesh. Introducing the arc-length s, the curves C_m^j and C_g^j are defined in parametric form by the points $\left(r_m^j(s), z_m^j(s)\right)$ and $\left(r_g^j(s), z_g^j(s)\right)$, respectively, in intervals of s to be defined. Moreover, the initial glass contour C_0 and that desired C_d are described by the points $\left(r_0(s), z_0(s)\right)$ and $\left(r_d(s), z_d(s)\right)$, respectively. The total length of the initial glass contour in the r-range of interest ($[0, r_i]$) is denoted by l_i and is computed according to

$$l_i = \int_0^{r_i} \left(1 + \left(\frac{dz_0}{dr}\right)^2\right)^{1/2} dr \,. \tag{1}$$

The end point of the initial glass contour $\left(r_0(l_i), z_0(l_i)\right)$ is displaced to $\left(r_e, z_e\right) = \left(r_0(l_i) + u_r^j\left(r_0(l_i), z_0(l_i)\right), z_0(l_i) + u_z^j\left(r_0(l_i), z_0(l_i)\right)\right)$ in the deformed glass geometry, where $\left(u_r^j(r,z), u_z^j(r,z)\right)$ is the displacement vector at the location (r, z) and iteration j. Thus, the length l_i in the initial glass geometry becomes l_e^j in the deformed geometry with

$$l_e^j = \int_0^{r_e} \left(1 + \left(\frac{dz_g^j}{dr}\right)^2\right)^{1/2} dr \,. \tag{2}$$

The curves C_m^j, C_g^j, C_d, and C_0 are now completely defined by the points $\left(r_m^j(s), z_m^j(s)\right)_{s\in[0,l_i]}$, $\left(r_g^j(s), z_g^j(s)\right)_{s\in[0,l_e^j]}$, $\left(r_d(s), z_d(s)\right)_{s\in[0,l_e^j]}$, and $\left(r_0(s), z_0(s)\right)_{s\in[0,l_i]}$, respectively. These curves are split into N equal intervals and the optimization loop proceeds on the $N+1$ corresponding control points.

Although the operator F can not be completely characterized, two features, illustrated in Figure 4, may be expected and assumed:

1. A point P_i initially located at $\left(r_0(s_i), z_0(s_i)\right)$ on the glass surface will be located around $G_i = \left(r_g^j(s_f), z_g^j(s_f)\right)$ in the deformed glass geometry (here, $s_i = i\frac{l_i}{N}$, $s_f = i\frac{l_e^j}{N}$ and the index i ranges from 0 to N). For example, a point located halfway through the initial glass contour may be expected to be located halfway through the deformed glass contour providing the curves remain reasonably smooth.

2. The modification of the mould at $M_i = \left(r_m^j(s_i), z_m^j(s_i)\right)$ only has a local effect on the initial glass surface at $P_i = \left(r_0(s_i), z_0(s_i)\right)$.

Based upon these assumptions, one can build a one to one operator F between $\left(r_m^j(s_i), z_m^j(s_i)\right)$ and $\left(r_g^j(s_f), z_g^j(s_f)\right)$, i.e.:

$$F\begin{Bmatrix} r_m^j(s_i) \\ z_m^j(s_i) \end{Bmatrix} \Rightarrow \begin{Bmatrix} r_g^j(s_f) \\ z_g^j(s_f) \end{Bmatrix}, \tag{3}$$

and construct an iterative scheme to identify the required mould geometry as follows

$$\begin{Bmatrix} r_m^{j+1} \\ z_m^{j+1} \end{Bmatrix} = \begin{Bmatrix} r_m^j(s_i) + \Delta_r^j(s_f) \\ z_m^j(s_i) + \Delta_z^j(s_f) \end{Bmatrix}, \tag{4}$$

where

$$\begin{Bmatrix} \Delta_r^j(s_f) \\ \Delta_z^j(s_f) \end{Bmatrix} = \begin{Bmatrix} r_d(s_f) - r_g^j(s_f) \\ z_d(s_f) - z_g^j(s_f) \end{Bmatrix}, \tag{5}$$

is the residual vector. After updating the location of the $N+1$ control nodes on the mould surface, the mesh of the upper and lower mould contour is reconstructed.

4. Mould design results

The optimization algorithm is applied to identify the required mould design which yields the desired plano-concave and bi-concave lenses described in the previous section. The mould design is optimized up to a radius r_i of 18 mm and the number of intervals N is chosen equal to

20. The only requirement on the number of nodes is that the number of control nodes should be sufficient to describe the curves accurately. The desired glass profile at room temperature is chosen as a first guess for the required mould shape. At each optimization loop, the same downward displacement which yields the desired centreline thickness is imposed on the upper mould and all other forming parameters apart from the unknown required mould contours remain identical.

Figures 5 and 6 plot the nodal distance from the desired to the deformed glass profiles, in the direction normal to the desired profile, for the bi-concave and the plano-concave lens designs, respectively. Of course, as the nodal residuals become smaller, the mismatch between the deformed and desired glass geometries decreases. These two figures confirm the success of the optimization algorithm since the best mould design from a total of 6 loops, allows a substantial drop in the average value of the nodal residuals and the micron target is almost achieved everywhere. Indeed for the flat surface of the plano-concave lens design, a reduction of the nodal residuals of almost two orders of magnitude is achieved. Iterating further does not reduce further the residuals as these become oscillatory, i.e. regions of decreasing and increasing residuals alternate. Finally, Figure 7 shows the lower profile of the plano-concave lens at the end of the process for each optimization loop. This figure clearly illustrates that this surface becomes flatter and flatter, and therefore gets closer and closer to the desired design, as the optimization algorithm proceeds.

5. Conclusions

A computer-aided optimization algorithm is presented in this paper for the mould design in high-precision compression moulding. Only a simplified model representative of the real industrial process is solved in the commercial finite element package ABAQUS. This model takes into account the multi-stage nature of the process, the thermo-mechanical coupling, the varying mechanical contact between the glass and the mould, and the complex rheology of the glass. The intuitive concept of the algorithm consists of computing at each optimization loop the mismatch between the final and desired lens profiles and using this information to update the previous mould design. Results for the mould design for a plano-concave and a bi-concave lens design confirm the feasibility of the method and its fast convergence rate. Indeed, only a few iterations are necessary to reduce the mismatch between the deformed and desired glass shapes to the targeted value of one micron. Although the true success of the optimization algorithm can only be assessed when applied to the real industrial process, this could provide a valuable alternative to other mould compensation technique.

Acknowledgements

The authors gratefully acknowledge the funding of the European Union through the MAGICAL project.

References

[1] Yi, A.Y**.** and Jain, A. Compression molding of aspherical lenses-a combined experimental and numerical analysis. *J. Am. Ceram. Soc.*, 2005, **88**, 579-586.

[2] Moreau, P., Lochegnies, D. and Oudin, J. Optimum tool geometry for flat glass pressing. *Int. J. Form. Proc.*, 1999, **2**, 81-94.

[3] Lochegnies, D., Moreau, P. and Guibaut, R. A reverse engineering approach to the design of the blank mould for the glass blow and blow process. *Glass Technol.*, 2005, **46**, 116-120.

[4] Agnon, Y. and Stokes, Y.M. An inverse modelling technique for glass forming by gravity sagging. *Eur. J. Mech. B-Fluids*, 2005, **24**, 275-287.

[5] Tool, A.G. Relation between inelastic deformation and thermal expansion of glass in its annealing range. *J. Am. Ceram. Soc.*, 1946, **29**, 240-253.

[6] Narayanaswamy, O.S. A model of structural relaxation in tempering glass. *J. Am. Ceram. Soc.*, 1971, **54**, 491-498.

[7] Scherer, G.W. Relaxation in glass and composites, Wiley, New York, 1986.

[8] Sellier, M. Optimal process design in high-precision glass forming. *Int. J. Form. Proc.*, 2006, **9**, 61-78.

Figure captions

Figure 1: Schematic view of the compression moulding process with the corresponding temperature treatment

Figure 2: Two-dimensional radial cross section of the finite element model of the glass/mould assembly for the plano-concave lens in the initial (left) and deformed (right) configurations

Figure 3: Two-dimensional radial cross section of the finite element model of the glass/mould assembly for the bi-concave lens in the initial (left) and deformed (right) configurations

Figure 4: Schematic description of the algorithm and the operator F which transforms the initial mould geometry into the final glass one

Figure 5: Normal distance (in mm) between the desired and deformed glass profiles in a direction normal to the desired profile for each of the control nodes and for the bi-concave lens design

Figure 6: Normal distance (in mm) between the desired and deformed glass profiles in a direction normal to the desired profile for each of the control nodes and for the bi-concave lens design

Figure 7: Lower lens profile at each optimization loop for the plano-concave design

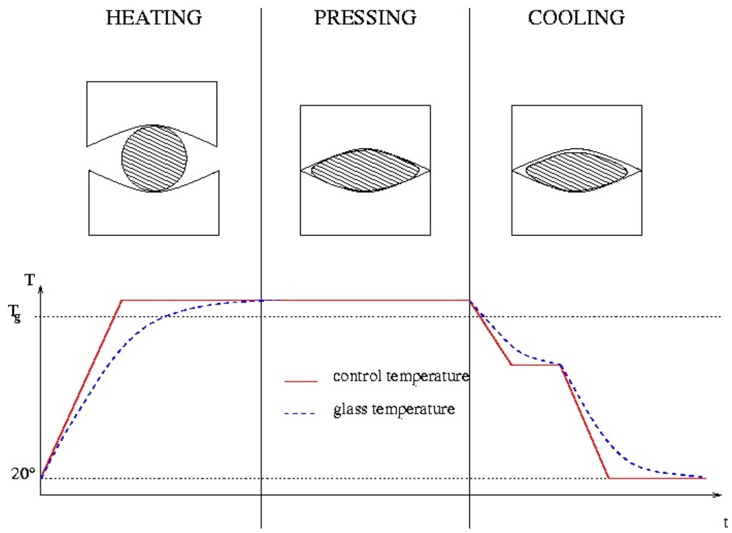

Figure 1: Schematic view of the compression moulding process with the corresponding temperature treatment

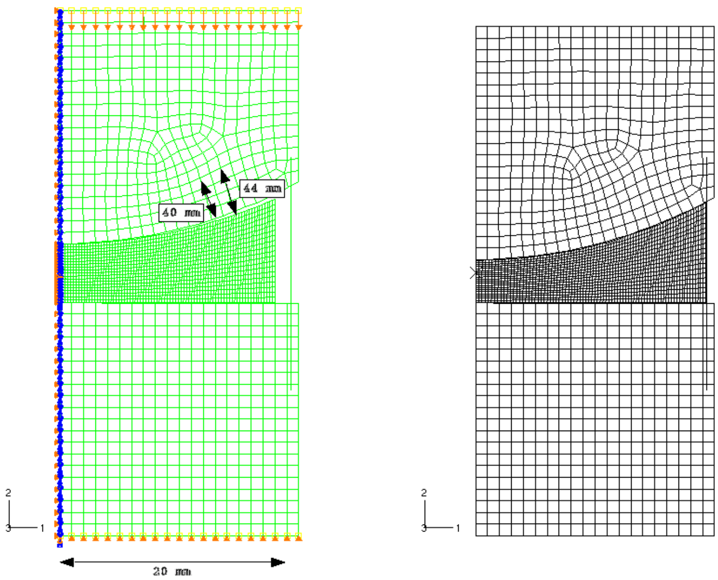

Figure 2: Two-dimensional radial cross section of the finite element model of the glass/mould assembly for the plano-concave lens in the initial (left) and deformed (right) configurations

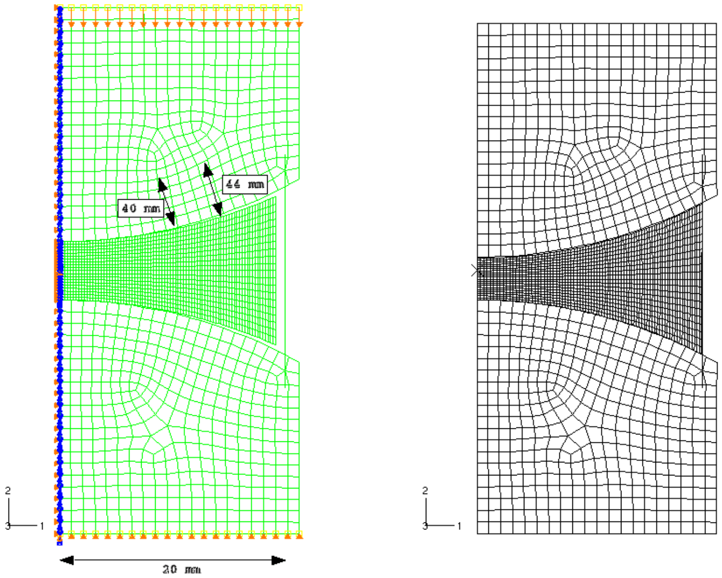

Figure 3: Two-dimensional radial cross section of the finite element model of the glass/mould assembly for the bi-concave lens in the initial (left) and deformed (right) configurations

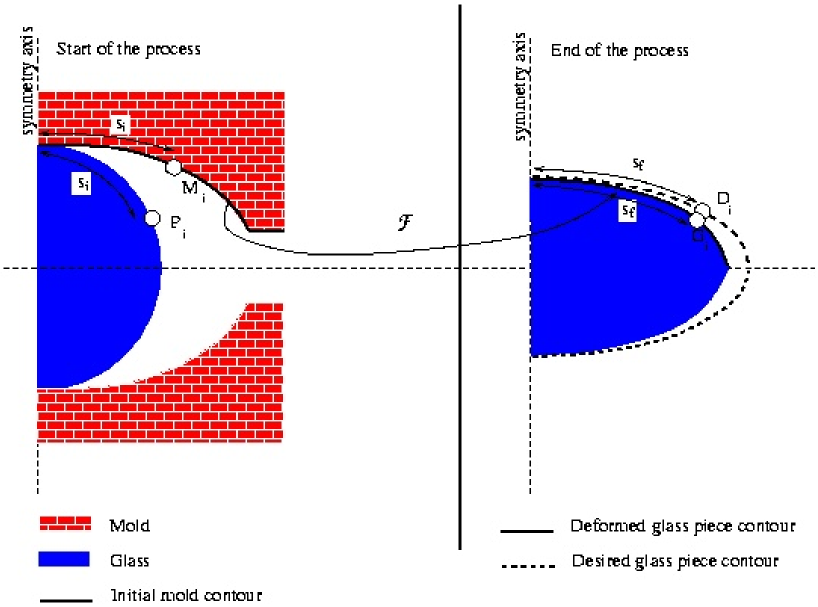

Figure 4: Schematic description of the algorithm and the operator *F* which transforms the initial mould geometry into the final glass one

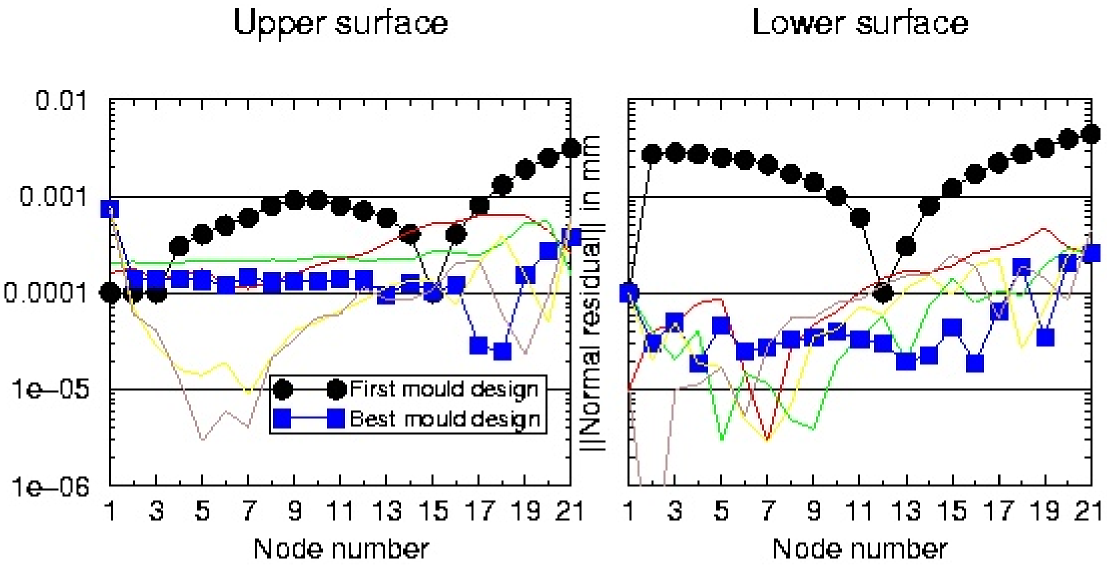

Figure 5: Normal distance (in mm) between the desired and deformed glass profiles in a direction normal to the desired profile for each of the control nodes and for the bi-concave lens design

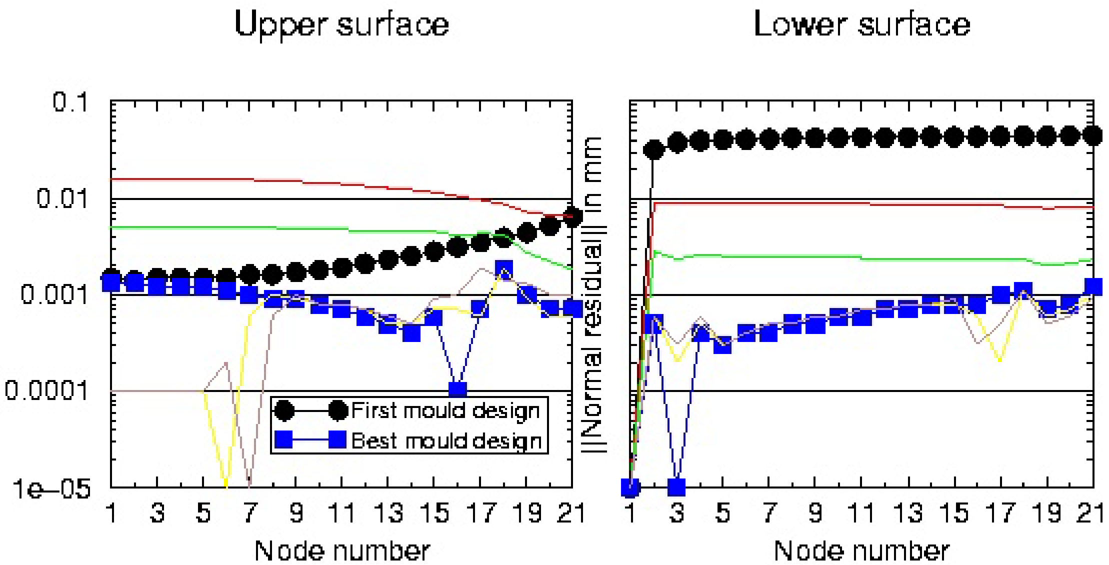

Figure 6: Normal distance (in mm) between the desired and deformed glass profiles in a direction normal to the desired profile for each of the control nodes and for the bi-concave lens design

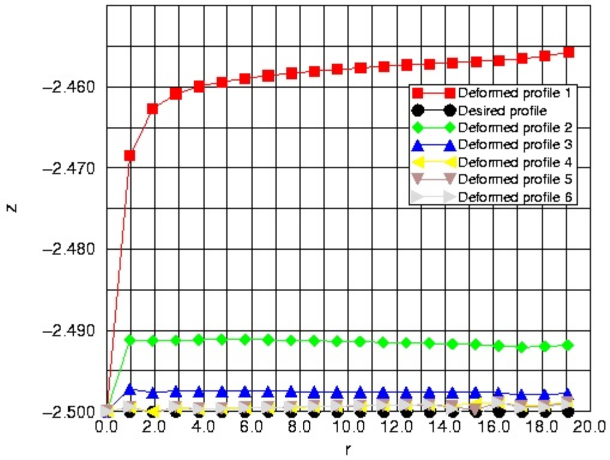

Figure 7: Lower lens profile at each optimization loop for the plano-concave design